A QUASI-ANALYTICAL MODEL TO PREDICT WATER QUALITY DURING THE OPERATION OF AN AQUIFER STORAGE AND RECOVERY SYSTEM

By

ALI SEDIGHI

A REPORT PRESENTED TO THE GRADUATE SCHOOL
OF THE UNIVERSITY OF FLORIDA IN PARTIAL FULFILLMENT
OF THE REQUIREMENTS FOR THE DEGREE OF
MASTER OF ENGINEERING

UNIVERSITY OF FLORIDA

2003

ACKNOWLEDGMENTS

I would like to offer my utmost appreciation to Dr. Kirk Hatfield, chairperson of my supervisory committee, who was much more than an advisor to me. He played a key role in guiding me with unlimited patience and energy and gave me all the support I could ask for. His experience and guidance have enlightened my education, as well as my life. I would also like to thank my committee members, Dr. Louis H. Motz and Dr. Michael D. Annable, for all of their valuable encouragements, ideas, and compassion throughout my study at the University of Florida. I am also grateful to all my previous professors at Sharif University of Technology in Tehran, Iran.

Behind the scenes was my loving girlfriend, Rachel Johnson, who rejoiced with me in good times and cheered me up in bad times. I thank her for her hard work in editing this paper and also her support and patience throughout the past year.

I am grateful to my friend, Harald Klammler, for all of his help, support, and great contribution to my work. I also wish to thank all my friends, especially Ali-Reza Kazemi, who has added richness to my life.

I am endlessly grateful to my parents, Parvin Bagherzadeh and Abdolvahab Sedighi, and my sister Vida for the emotional and financial support afforded me throughout my life.

TABLE OF CONTENTS

LIST OF FIGURES

Abstract of Thesis Presented to the Graduate School
of the University of Florida in Partial Fulfillment of the
Requirements for the Degree of Master of Engineering

A QUASI-ANALYTICAL MODEL TO PREDICT WATER QUALITY DURING THE OPERATION OF AN AQUIFER STORAGE AND RECOVERY SYSTEM

By

Ali Sedighi

August 2003

Chair: Kirk Hatfield
Major Department: Civil and Coastal Engineering

Aquifer Storage Recovery (ASR) is defined as the storage of freshwater in an aquifer by injecting water through the wells during wet periods for subsequent retrieval from these same wells during dry periods. The freshwater forms a bubble of injected water within the aquifer around the ASR well, and it can be retrieved when needed to meet seasonal, long-term, emergency or other demands. During the past ten years, ASR technology has evolved from merely a concept to a proven, cost-effective and environmentally desirable water management tool.

The objective of this paper is to develop an analytical model to determine recovered water quality based on the position of the injected water, surrounded by the ambient water of the aquifer. Injected water and ambient water are characterized as two separate zones by the differing concentrations of specific dissolved species. When these two zones are introduced to each other, a transition zone is created across which the concentration varies. The transition between these two zones is modeled by creating a

distribution of hydraulic conductivity across the depth of the aquifer. Thus, in a layer with a constant value of hydraulic conductivity, the transition zone is replaced by a sharp front, which, while moving, continuously separates the two zones with different concentrations. By keeping track of the front position during injection, storage, andrecovery, we can obtain the fraction of injected water contained in the pumped water from the angle of the injected water body surrounding the well; thus, the concentration of recovered water will be a number between the concentration of injected water and the concentration of ambient water.

To validate this analytical model, the results are compared with numerical models, using MODFLOW-96 and MT3DMS packages. The running time for this analytical model is less than 10 percent of the running time in existing numerical models. Also, considering the simple way of introducing input data, it can be superior to the existing numerical models.

CHAPTER 1
INTRODUCTION

Population growth during the past few decades has accelerated the demand on both surface and groundwater supply. Aquifer Storage and Recovery (ASR) is an important component of groundwater management. ASR is defined as the storage of freshwater in an aquifer through the wells during periods when surface supplies are plentiful for subsequent retrieval from these same wells during dry periods. The injected water forms a bubble within the aquifer around the ASR well, and can be retrieved when needed to meet seasonal, long-term, emergency or other demands. The potential for seasonal storage and drought protection have made ASR one of the most promising storage methods for potable, surface and reclaimed water.

The term "Aquifer Storage Recovery" was coined by David G. Pyne in 1983 when the first ASR system in Manatee County, Florida, began successful operation (Pyne, 2003). As of January 2003, fifty-six ASR systems are believed to be operational in the United States, 12 of which are located in Florida. This compares to the three ASR systems in 1983. Most systems are storing treated drinking water. At least 100 other ASRs are in various stages of development, ranging from planning to operational startup. Figure1-1 shows the location of ASR systems in the North America as of January 2002. Other systems are known to be operating in the United Kingdom, Canada, Australia and Israel. ASR development programs are underway in several other countries, including the Netherlands, New Zealand, Thailand, Taiwan, Saudi Arabia, and Kuwait (Pyne, 2002 and Lloyd, 2001).

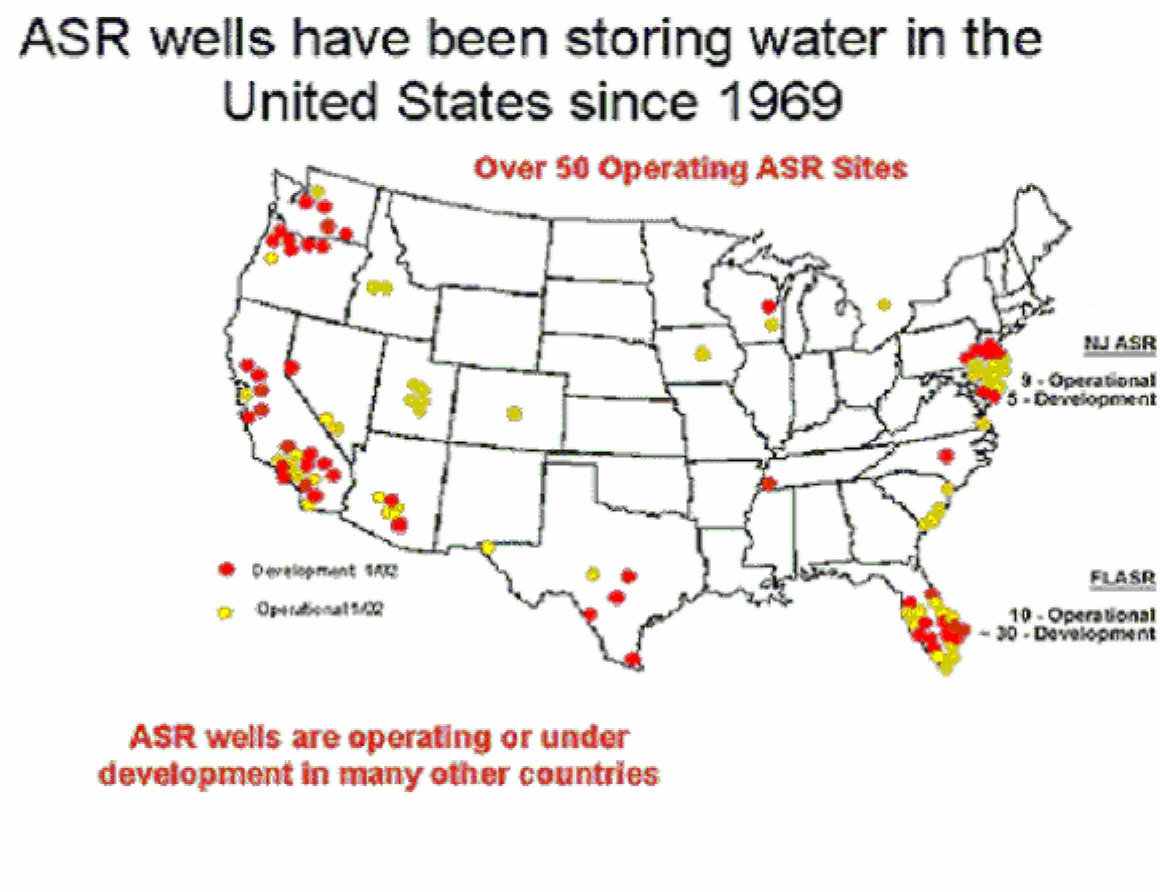

Figure 1-1. Distribution of operational and under development ASR systems in North America (Pyne, 2003).

The Comprehensive Everglades restoration Plan (CERP) proposes to use as many as to 333 ASR wells to store as much as 1.6 billion gallons of freshwater per day to ensure the quantity of water available to the Everglades, improve water quality conditions in Lake Okeechobee, and prevent damaging releases of freshwater to coastal estuaries (Figure 1-2). Some of this water would also be available to support surrounding agriculture and to protect urban wells located near the coast from salt-water intrusion.

Muniz and Ziegler (1994) detail the feasibility, construction, testing and initial operation of the Boynton Beach, Florida ASR well. This case study is of particular value to the CERP because it is within 20 miles of proposed ASR wells in CERP. The first step in hydrogeologic characterization of the site was the boring of pilot holes. Geologic logs from the pilot holes were used to assist in correlating formation samples to identify specific lithologic boundaries design. Cycle testing was successful in determining operational performance, evaluating potential recharge and recovery of treated drinking water, confirming that recovered water met drinking water standards, and estimating the hydraulic performance of the storage zone.

Successful experience at most monitoring sites has confirmed that ASR is not only practical, but cost-effective for storing water deep underground. However, Nguyen and Mueller (1996) recommend that all ASR projects should be considered only on an experimental basis in the initial phase to allow collection of valuable data to assess the aquifer characteristics and the quality of the native water in the storage zone.

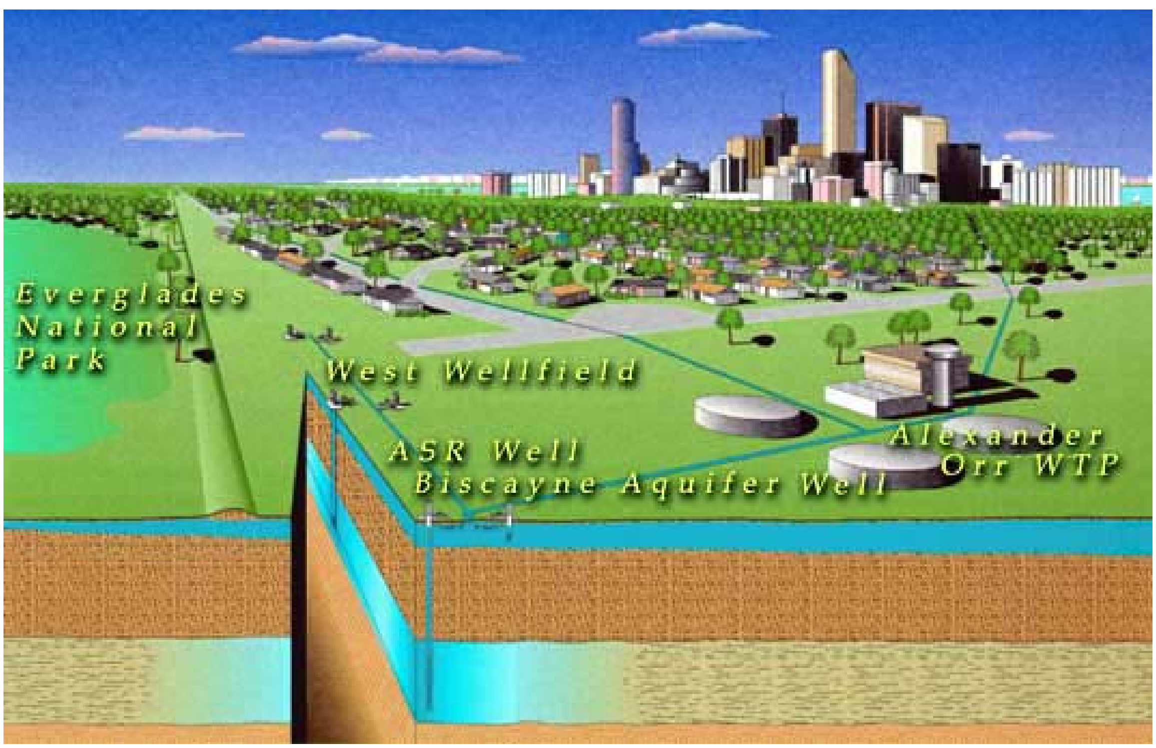

Figure 1-2. Miami-dade County, Florida, recovers water stored in a 1000 to 1300 foot deep (300-400 m) brackish limestone aquifer (Pyne, 2003).

Applications and Benefits of ASR Technology

The primary driving force behind the current rapid global implementation of ASR technology is water supply economics. ASR provides a cost-effective solution to many of the world's water management needs and can usually meet water management needs at less than half the capital cost of other water supply alternatives (Pyne, 2002). Large water volumes are stored deep underground, reducing or eliminating the need to construct large and expensive surface reservoirs. ASR is most commonly used in conjunction with the potable water treatment systems for purposes of storing excess treated water in the ground. Water treatment plants typically face their peak demand only during short periods each year. An ASR can replace the storage capacity that otherwise must be built into a plant's surface facilities; hence, it can minimize capital and operating costs. Wells can be located where most needed and because wells require little land, the costs of large land acquisitions are avoided.

ASR also results in less water lost. Some areas have seasonally abundant water resources (like Florida) but few good places to store the water. Evapotranspiration and seepage losses are high in surface reservoirs, whereas for underground storage these two problems are insignificant. ASR systems could potentially allow for multi-year storage, whereas evaporation during severe droughts limits the ability of reservoirs to provide similar long-term storage.

Several benefits can be cited with respect to the adoption of ASR systems. First, most obviously these systems can be used to store water when the supply is abundant and the water quality is good for purposes of recovering it later during emergencies or times of water shortage, or when source water quality is poor. Second, during the recharge cycle, groundwater levels can then be restored where aquifers have experienced long term declines in water levels due to heavy pumping to meet increasing urban and agricultural water needs. Finally, ASR is generally viewed as an environmentally good alternative to surface water reservoirs because they reduce or eliminate the need for dam construction, and they provide for reliable water supplies through the diversion of flood flows instead of low flows.

In addition to meeting increased water demands, ASR plays a role in solving the challenges of wet weather surface flows and groundwater and wastewater management. For example, as urban development continues, the area of impermeable ground cover continues to expand, raising the level of surface runoff and its attendant problem of erosion, silting, and pollution. Stormwater serves a better purpose when it can be captured and safely reintroduced to the aquifer. In addition, with saltwater intrusion threatening drinking water supplies in coastal areas, ASR injection wells can create water barriers that protect vulnerable aquifers. Finally, ASR can also be used to recycle treated wastewater (Missimer et al. 1992).

ASR applications, particularly in Florida, are for seasonal water storage, but other applications include long term water storage or water banking from wet years to drought years, emergency water storage, restoring water levels in depleted aquifers, controlling subsidence, maintaining pressures and flows in water distribution systems, improving water quality, reducing the cost of water system expansions, maintaining minimum flows and levels, and many other applications. Increasingly, ASR is being considered for development of Strategic Water Reserves to provide water supply security from terrorism or warfare (Reese, 2002 and Pyne, 2002).

Research Objective and Scope

The objective of this research was to predict water quality changes during the operation of an ASR system. The efficiency of ASR operations is dependent on the volume of stored water recovered. The recovered volume depends on transient changes in water quality that result from ASR operations. Tools developed to better predict water quality changes during ASR operations could be used to optimize the management of ASR systems. To meet the above stated research objective, a quasi-analytical model has been developed. In this model, the recovered water quality is calculated based on the simulated position of the injected volume of water with respect to the ambient water of the aquifer, the quality of the injected water, and the quality of the ambient groundwater. To validate the quasi-analytical model, results are compared to the well-known numerical models, MODFLOW-96 (Harbaugh and McDonald, 1996a and 1996b) and MT3DMS (Zheng and Wang, 1999).

CHAPTER 2
LITERATURE REVIEW

ASR Modeling

Numerical models such as MODFLOW-96 (Harbaugh and McDonald, 1996a and 1996b) and MT3DMS (Zheng and Wang, 1999) and SEAWAT (Guo and Langevin, 2002) are available to simulate the movement of injected water through an ASR well and to predict the transient quality of recovered water. To perform these simulations, the spatial and temporal scales of numerical discretization must be sufficiently small to minimize numerical dispersion and preserve mass balances on simulated water quality parameters. The high level of discretization and the associated increased computational demands required may all but preclude direct application of numerical codes except over small and unstratified aquifer domains. Analytical models potentially offer computation efficiencies for simulating transport through homogeneous aquifers not easily afforded through numerical transport models.

Analytical models were developed to study movement of injected water in the aquifer. Muskat (1937) considered the steady flow pattern produced by a single pumping well near an equipotential boundary, while Bear (1979) studied the shape of the advancing front separating the indigenous water of a confined aquifer from a body of water injected into it through a well at the origin. However, Muskat and Bear did not seek to predict water quality during all operational phases of an ASR system. Their models do provide insight into the groundwater velocity field that ultimate plays a significant role in the transport of dissolved constituents.

Nelson (1978) developed a semi analytical approach that provides location/arrival time distributions and location/outflow quantity distributions at critical outflow boundaries of the system. This model assumes that the concentration distribution at the beginning of the simulation is known.

Javandel and others (1984) developed a particle-tracking model to show how spatial distribution in concentration versus time data for a single injection well reaches any desired outflow boundary. This model calculates the time it takes for a particle to flow to a pumping well given all pumping and injection rates. It is required to construct flow patterns and then use them to identify the locations of any contaminant fronts for various values of time.

Javandel and Tsang (1986) developed the previous model to determine the capture zone of multiple wells. The new model can assist in the determination of the optimum number of pumping wells, their rates of discharge and locations, such that further degradation of the aquifer is avoided.

Ahlfeld (1999) used particle tracking techniques to develop an optimization formulation for designing groundwater plume control systems.

The limitation of these models is the inability to account for dispersion. The particle-tracking model developed by Javandel and others (1984) can be applied to predict water quality in an ASR system. However, the quasi-analytical model developed herein is simpler since there is no need to construct flow patterns in the aquifer. The quasi-analytical model does not simulate the transport of dissolved solutes but determines the transient fraction of ambient groundwater recovered during the ASR extraction phase. Because convective/dispersive transport process are not explicitly simulated, the quasi-analytical model is limited to simulating water quality changes at the ASR well and during the recovery phase; however, these simulations can be achieved at significant computational efficiencies over traditional numerical transport models. To emulate the effects of hydrodynamic dispersion, these simulations are performed as if the aquifer were stratified and the horizontal hydraulic conductivity varied vertically in a statistically defined manner.

Hydraulic Factors and Characteristics of ASR Systems

For most ASR systems, storage volumes range from as small as 13 million gallons (MG) in individual ASR wells to as much as 2.5 billion gallons (BG) or more in large ASR well fields. The shallowest depth to the top of a storage zone is about 200 feet while the greatest depth to the base of an ASR storage zone is 2600 feet. The thinnest storage zone is about 50 feet while the thickest is about 1300 feet. Natural water quality in storage zones ranges from freshwater that is suitable for drinking without treatment to brackish water with total dissolved solids concentrations up to about 5000 mg/l. Most sites have one or more natural water quality constituents that are unsuitable for direct potable use except following treatment. Such constituents may include iron, manganese, fluoride, hydrogen sulfide, sulfate, chloride, radium, gross alpha radioactivity, and other elements that are typically displaced by the stored water as the bubble is formed underground.

Arthur et al (2001) studied the geochemical aspects of the Florida Aquifer Storage and Recovery system. Results of this study indicate that chemical variability (including isotropy) exists within groundwater and carbonate of the Floridan aquifer system which may result site-specific geochemical processes affecting ASR well performance and water quality. Also, as oxygen-rich surface waters are injected into Floridan aquifer system, trace metals such as arsenic (As), iron (Fe), manganese (Mn) and uranium (U) are mobilized (chemically leached) from the carbonate rocks and withdrawn during recovery. Therefore, some of the periods of higher metals concentrations in the recovered water are short-lived, depending on the duration of the injection, storage, and recovery cycles. Their results confirm that understanding water-rock geochemical interactions are important to the continued success of ASR in Florida.

Merritt (1985) studied the relationship of recovery efficiency to the hydrogeologic conditions that could prevail in brackish artesian aquifers. The principal tool of investigation used in his study was the INTRA model which has a variety of potential applications to variable-density solute-transport problems. He found that a loss of recovery efficiency was caused by (1) processes causing mixing of injected freshwater with native saline water (hydrodynamic dispersion), (2) process causing the more or less irreversible displacement of the injected freshwater with respect to the well (background hydraulic gradient, interlayer dispersion, buoyancy stratification), or (3) processes causing injection and withdrawal flow patterns to be dissimilar (directionally biased well-bore plugging, dissimilar injection and withdrawal schedules in multiple well systems).

Success or failure of an ASR system is controlled by a wide variety of factors that are related to hydrogeologic conditions, well design, and operational management. Some of these factors are (Bear, 1979, Missimer et al, 2002, and Reese, 2002):

- Natural gradient
- Aquifer porosity
- Hydrodynamic dispersion (which includes the effects of molecular diffusion and mechanical dispersion)

- Confinement of the aquifer
- Aquifer permeability and its distribution
- Aquifer transmissivity
- Aquifer thickness
- Ambient water quality and density
- Injected water quality
- Desired extraction water quality
- Injection and recovery flow rates
- Duration of different periods (injection, storage, and recovery)
- Frequency of cycles and storage period at the end of each cycle

Recovery efficiency is significantly affected by the downgradient movement of injected water due to the background hydraulic gradient. The average velocity of ambient flow is a function of the hydraulic conductivity and porosity as well as the natural gradient.

The degree of mixing between the injected water and native water and the width of transition zone is controlled by hydrodynamic dispersion, which in turn is a reflection of the degree of spatial variability in aquifer conductivity. Some sites show minimal mixing on the initial cycle, and, if the natural hydraulic gradient in the aquifer is small, after two or three cycles the same volume stored the quality of recovered water is quite stable. On the other hand, some sites show substantial mixing, suggesting that even with a small hydraulic gradient a very large water quality transition zone would be encountered to achieve 100% recovery.

If the storage zone is not well confined, injected water may move upward or downward out of the storage zone, or ambient water may move vertically into the storage zone during recovery. Most sites use confined or semi confined aquifers for storage; however, at several sites the aquifer is unconfined. Sometimes a subsurface zone must have barriers to contain stored water.

Permeable sediments or rock must be present to allow flow of water through the aquifer. The hydraulic conductivity or permeability distribution in the storage zone greatly influences the recovery efficiency. Mechanical dispersion is related to the distribution of permeability within the storage zone. Higher permeability can cause higher dispersive mixing, and hence lower recovery efficiency. As a result, a sandy aquifer with relatively uniform permeability could have better recovery efficiency since the primary component of dispersion results from flow through intergranular pore space alone. However, suitable storage zones include a wide variety of geologic settings such as sand, sandstone, gravel, limestone, dolomite, glacial drift aquifers, and basalt.

The transmissivity of an aquifer has an effect on the ability to recover injected freshwater. The transmissivity of the selected aquifer must be high enough to allow water to be injected and recovered at sufficient rates to allow the system to economically achieve the design goals. However, the transmissivity must be low enough to allow the injected water to be recovered without losing it in the aquifer as a result of migration under natural gradient condition. Therefore, the transmissivity must lie within a range of values depending on the desired pumping rates and the recoverability percentage (Missimer et al, 2002).

Recovery efficiency is greater in a thin aquifer than in a thick aquifer because of the lower vertical extent of the transition zone along which mixing occurs. However, this effect can be partially offset by increasing the volume of water recharged during a cycle. Minimizing the thickness of the storage zone within a thick aquifer can also be beneficial depending on the aquifer's distribution of vertical hydraulic conductivity (Reese, 2002).

The ambient concentration in the aquifer is of primary importance in controlling recovery efficiency. This will be addressed later when the model is being developed. Buoyancy can play a significant role in the success or failure of an ASR system. In some places, like South Florida, ASR is mostly used to store water in an aquifer that contains brackish water. Therefore, the density difference between freshwater and ambient water is substantial and the greater the differential in density, the faster freshwater will move upward in an aquifer. When the density differential is relatively small, the issue of density-driven water movement is not significant because the lower vertical hydraulic conductivity compared to horizontal hydraulic conductivity tends to reduce the effect (Missimer et al, 2002).

Increasing the injection and recovery flow rates would dominate the effect of freshwater displacement during injection and recovery. There is a portion of injected freshwater which has moved downgradient and can never be recovered. By increasing the recovery flow rate, we can reduce this volume of unrecoverable water. However, injection and recovery rates are site-specific parameters; therefore they must be confirmed at each well cluster location (Bouwer, 1996).

Martin and Dean (2001) detail the presence of known fractures in the Floridan aquifer system of north-central Florida determined via dye trace studies and cave diving explorations. They also detail how this extensive fracture system, and the resulting simultaneous conduit and matrix groundwater flow, create the requirement for dual-porosity groundwater modeling. The ASCE Standard Guidelines for Artificial Recharge of Groundwater (2001) explains that determination of the critical injection pressure is the key factor to prevent hydrofracturing and it suggests a range of **0.2-0.6h** depending on site specific conditions, where **h** is the head necessary to raise the potentiometric surface at the recharge well to the ground surface.

Increasing the duration of different phases during the operation of an ASR system would decrease the recovery efficiency. The longer the duration of each phase, the more the displacement of injected freshwater. Also, dispersion and mixing would appear more during the long periods of injection, storage and recovery. Recovery efficiency would improve with repeated cycles because some of the recharged water from a previous cycle is left in the aquifer (especially when natural hydraulic gradient is low), and during the next cycle, recharged water mixes with water of a lower concentration.

There are still some uncertainties about ASR systems, and an additional step in the path forward would be a better understanding of the processes by which changes in water quality occur during ASR operation. This will help determine the feasibility of using ASR on a much larger scale as proposed in Comprehensive Everglades Restoration Plan (CERP).

Operation of the Aquifer Storage and Recovery Systems

ASR wells are evaluated and operated through a cyclical process. Each cycle includes periods of injection (recharge), storage, and then recovery with each period lasting days or months. During the injection period, a portion of the excess available surface water supply is treated and injected via the ASR well into a deep and mostly confined aquifer, creating a large reservoir of stored water that slowly displaces the ambient groundwater. Figure 2-1 shows the position of injected water in the aquifer after the recharge cycle.

Due to the natural hydraulic gradient in the aquifer, injected water moves down gradient throughout the phases of injection, storage and recovery. When the recharge water that is characterized by concentrations of multiple dissolved solutes is introduced into an aquifer with indigenous water comprised of different solutes and concentrations, a transition zone is created across which solute concentrations vary (Bear, 1979). The transition zone separates ambient water from the injected freshwater bubble.

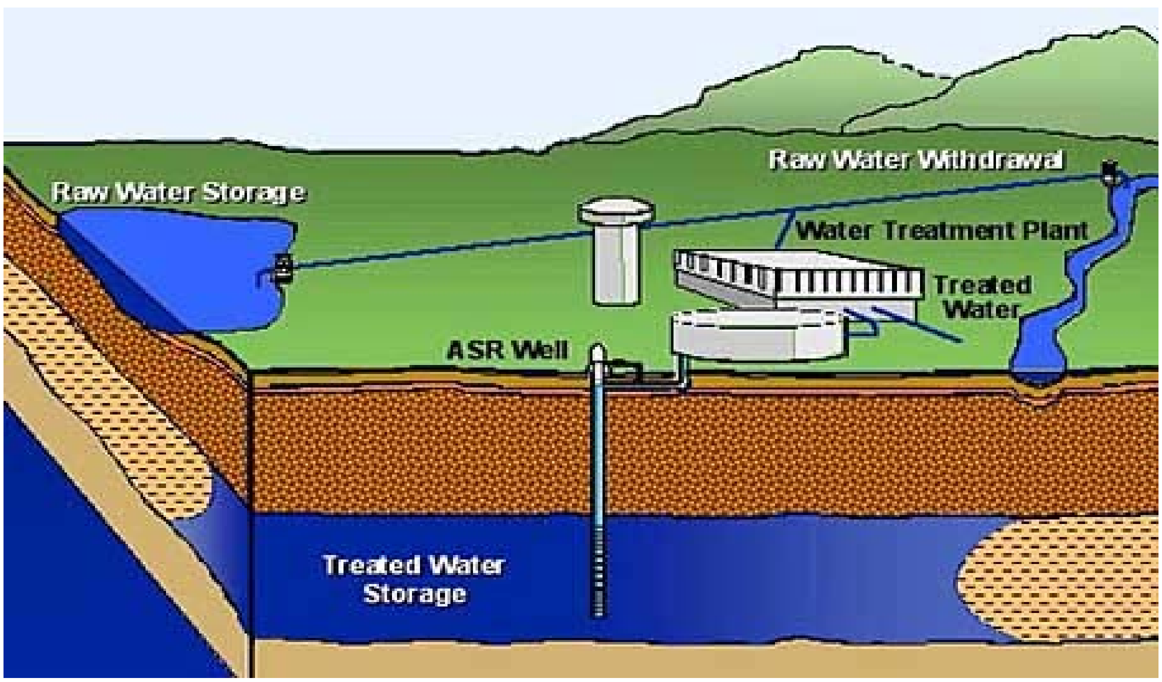

Figure 2-1. Captured water from rainfall is treaded and pumped into an aquifer through ASR wells (Pyne, 2003).

Figure 2-2 shows the position of fresh water and transition zone at the end of the storage phase. As shown in Figure 2-2, the freshwater reservoir is asymmetrically distributed around the ASR well to indicate that it has migrated under natural gradient conditions. The degree of mixing between the injected and ambient water and the width of the transition zone increases with the length of flow of the advancing front and is controlled by hydrodynamic dispersion. Often, it is the case that the transition zone can be neglected, because it is narrow relative to the length dimension of the areas (or volume) occupied by the injected water (Bear, 1979).

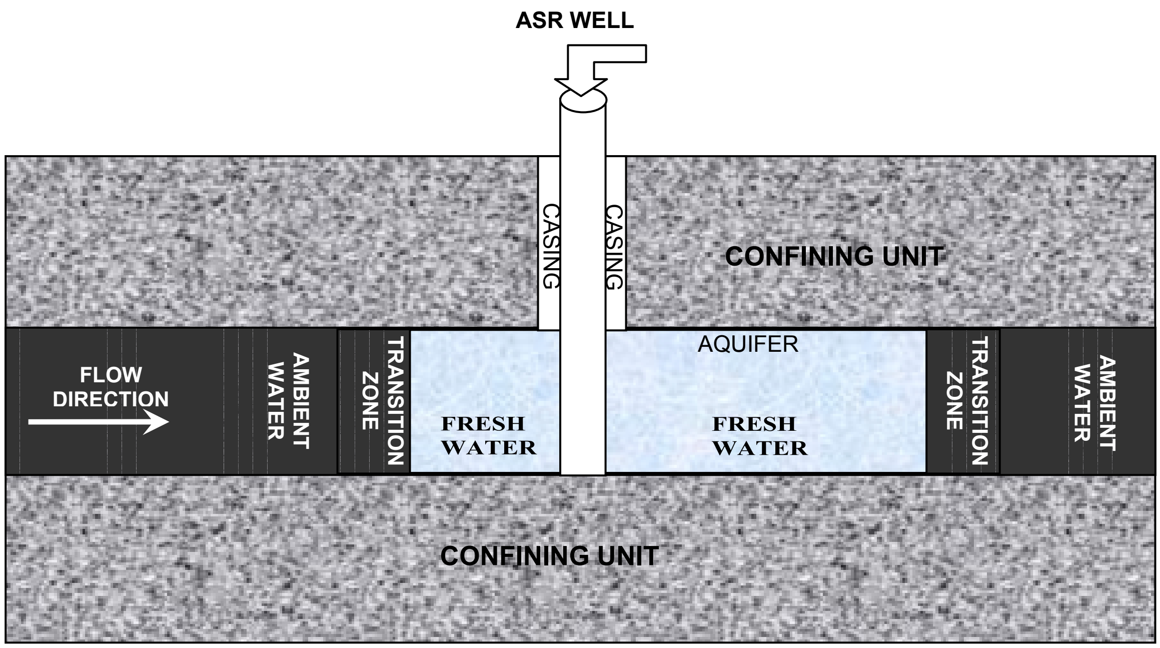

Figure 2-2. After storage period, transition zone is created and it separates freshwater from ambient water in the confined aquifer. Also injected freshwater has moved downgradient due to the natural groundwater velocity.

CHAPTER 3
ASR MODEL

This chapter focuses on two objectives. The first is to develop a quasi-analytical model to predict the quality of water recovered during the operation of an ASR system. The second objective is to validate the model by comparing simulation results of test cases against a numerical simulation generated using MODFLOW-96 (Harbaugh and McDonald, 1996a and 1996b) and MT3DMS (Zheng and Wang, 1999) packages.

Analytical Statement of Front Movement

The assumed conceptual model of an ASR system operating in homogeneous confined aquifer is that of a fully screened well, uniformly recharging or extracting water over the entire thickness of the aquifer, **L**. During extraction and recharge, stored water is continuously under the influence of regional hydraulic gradient. It is conceptually assumed that the regional aquifer flow is uniform and of a steady specific discharge **q** that is proportional to the regional hydraulic gradient in an aquifer that is both homogeneous and of constant thickness. Thus,

$$q = -K \frac{d\varphi}{ds} \tag{3-1}$$

in which **K** is the aquifer hydraulic conductivity [L/T]; φ is the hydraulic head [L], and **s** is the primary direction of groundwater flow [L]. This natural gradient flow is considered here to describe the horizontal displacement of water injected at the ASR well.

To model the geometry of the advancing front separating the indigenous water of a confined aquifer from a body of injected water during the operation of an ASR system, the total injection time is discritized into **n** subintervals of **Δt**.

$$T_i = \sum_{1}^{n} \Delta t \qquad (3\text{-}2)$$

where $\mathbf{T_i}$ is the duration of the injection cycle [T]. The radius of the cylindrical volume of injected water after time **Δt** is C such that:

$$ri_1 = C = \left(\frac{Q_i \Delta t}{L \eta \pi} \right)^{\frac{1}{2}} \qquad (3\text{-}3)$$

of which $\mathbf{Q_i}$ is the injection flow rate [L3/T]; and **η** is the effective porosity of the aquifer. Of the water stored in the aquifer, it may be assumed from equation (3-3) that a plan view of the injected bubble may be represented as follows:

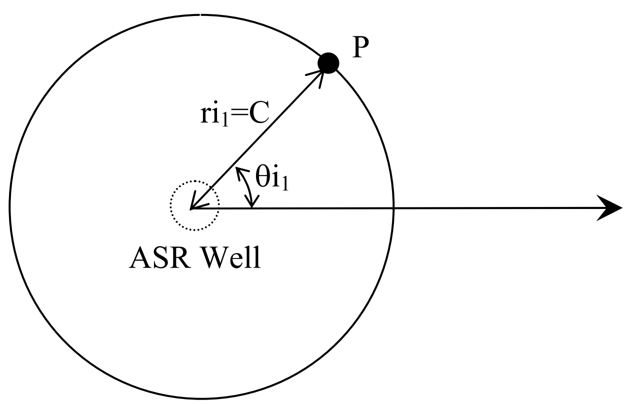

Figure 3-1. Plan view of the injected water after time Δt and before movement.

Differences in density and viscosity between injected and ambient waters are neglected, such that the front separating injected from ambient waters of the aquifer is composed of all particles leaving the ASR well at t = 0. Clearly, it is necessary to monitor the migration of multiple fluid particles such that their positions may be used to reconstruct the geometry of the front. Thus, moving multiple fluid particles and tracking their positions over successive time intervals leads to an assessment of the position of the front at any time. In this development, the position of point **P** is followed where this point is situated on the boundary between the injected water and the ambient groundwater.

After time **Δt** and under natural gradient conditions, it is assumed that the cylindrical volume of the stored water is displaced down gradient a distance $\mathbf{B_i}$ from the ASR well. The position of the injected bubble at this time is shown in Figure 3-2.

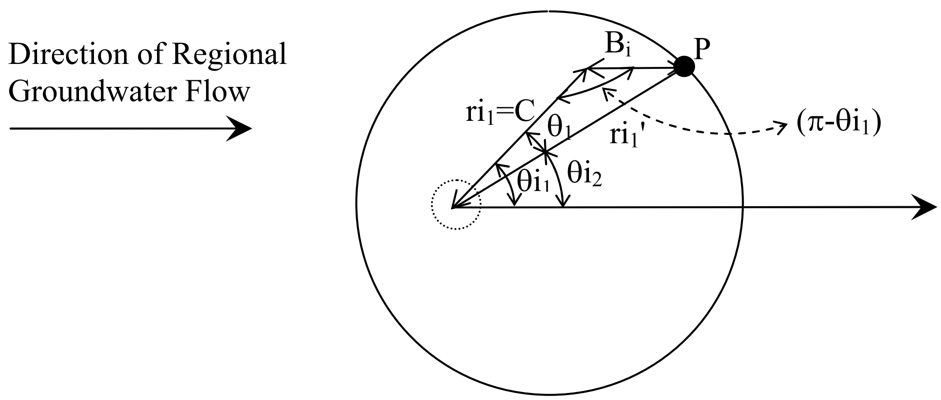

Figure 3-2. Plan view of the injected water after time Δt and after movement.

The displacement distance $\mathbf{B_i}$ is estimated from equation (3-4):

$$B_i = \frac{q\Delta t}{\eta} \tag{3-4}$$

The relation between parameters of Figure 3-2 can be written as:

$$ri_1' = \sqrt{ri_1^2 + B_i^2 - 2ri_1 B_i \cos(\pi - \theta i_1)} \tag{3-5}$$

or:

$$ri_1' = \sqrt{ri_1^2 + B_i^2 + 2ri_1 B_i \cos\theta i_1} \tag{3-6}$$

where $\boldsymbol{\theta i_1}$ is specified and ri_1 is obtained from equation (3-3). In addition, there is:

$$\frac{\sin\theta_1}{B_i} = \frac{\sin(\pi - \theta i_1)}{ri_1'} \tag{3-7}$$

$$\therefore \qquad \sin\theta_1 = \frac{B_i}{ri_1'}\sin\theta i_1 \qquad (3\text{-}8)$$

$$\therefore \qquad \theta_1 = Arc\sin(\frac{B_i}{ri_1'}\sin\theta i_1) \qquad (3\text{-}9)$$

$$\therefore \qquad \theta i_2 = \theta i_1 - \theta_1 = \theta i_1 - Arc\sin(\frac{B_i}{ri_1'}\sin\theta i_1) \qquad (3\text{-}10)$$

As freshwater injection continues at the constant rate of $\mathbf{Q_i}$ for another time interval of $\mathbf{\Delta t}$ (total time=$2\Delta t$), the injected fresh water displaces the stored bubble in a manner as depicted in Figure 3-3. The total area is twice the area at $t = \Delta t$; thus, the shaded area in Figure 3-3 is equal to $\pi\mathbf{C}^2$.

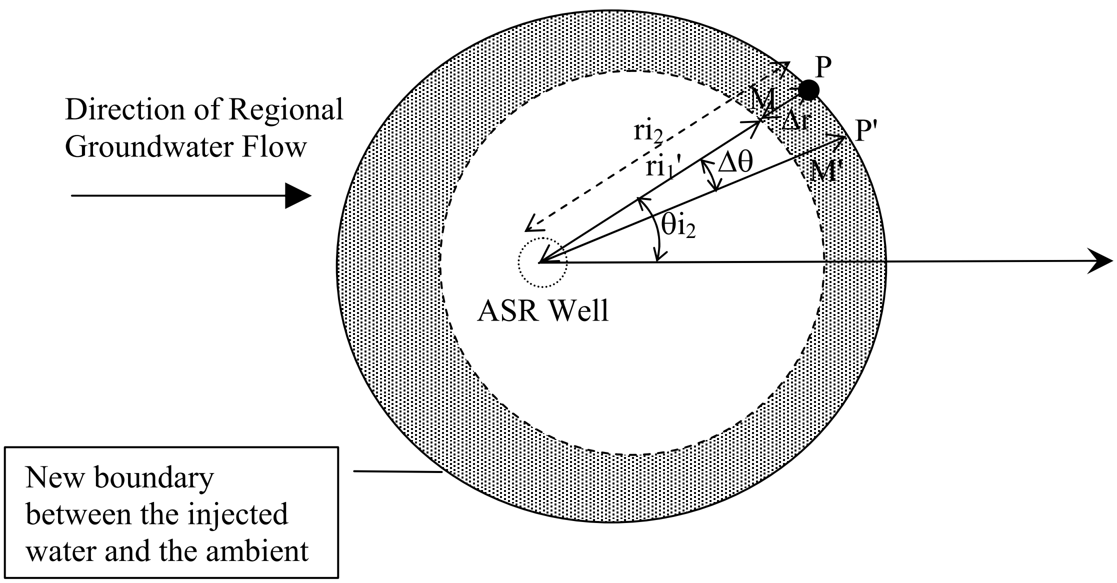

Figure 3-3. Position of the injected water after time $2\Delta t$ and before movement.

From Figure 3-3, $\mathbf{ri_2}$ equals the new distance of point **P** from the center of injection well:

$$ri_2 = ri_1' + \Delta r$$

For a small value of Δθ it can be assumed that arcs **PP'** and **MM'** define circles; thus:

$$\pi(ri_2^2 - ri_1'^2)\frac{\Delta\theta}{360} = \pi C^2 \frac{\Delta\theta}{360} \quad (3\text{-}11)$$

$$\therefore \quad ri_2 = \sqrt{C^2 + ri_1'^2} \quad (3\text{-}12)$$

Figure 3-4 shows the shape of the advancing front after time=2Δt**.** Again, under natural gradient conditions, the volume of the fresh water is displaced down gradient a distance $\mathbf{B_i}$ from the ASR well from its location in Figure 3-3. Thus,

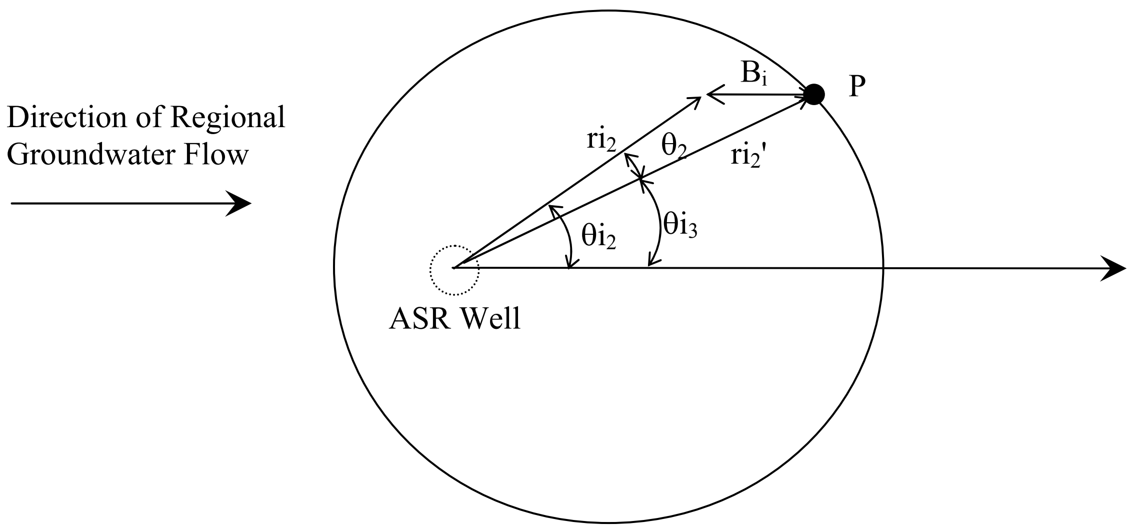

Figure 3-4. Position of the injected water after time 2Δt and after movement.

Similar to what was needed to obtain the value of $\mathbf{ri_1'}$ and $\mathbf{\theta i_2}$ in equations (3-6) and (3-10), the distance of point **P** from the injection well is equal to $\mathbf{r_2'}$ where:

$$ri_2' = \sqrt{ri_2^2 + B_i^2 + 2ri_2 B_i \cos\theta i_2} \quad (3\text{-}13)$$

$$\theta i_3 = \theta i_2 - \theta_2 = \theta i_2 - Arc\sin\left(\frac{B_i}{ri_2'}\sin\theta i_2\right) \quad (3\text{-}14)$$

All the parameters on the right hand side of these equations are known. Therefore the polar coordinates with respect to the ASR well or (ri_2', θi_3) can be determined for point **P** located on the injected/ambient water interface.

Assuming the injection process continues for successive time intervals of **Δt** until $\sum \Delta t = T_i$, the displacement of point **P** along with a sufficient number of fluid particles (points) on a front (different values for θi_n in Figure 3-1) maybe traced or followed such that the position of the front can be ascertained. By considering the displacement of multiple particles during small time intervals of **Δt**, the coordinates are known for several points like **P** that define the front at the end of injection time (T_i). Due to symmetry of the injected volume, values of **θi** between **0** and π also represent the values of **θi** between **0** and **-π** (**-θi**).

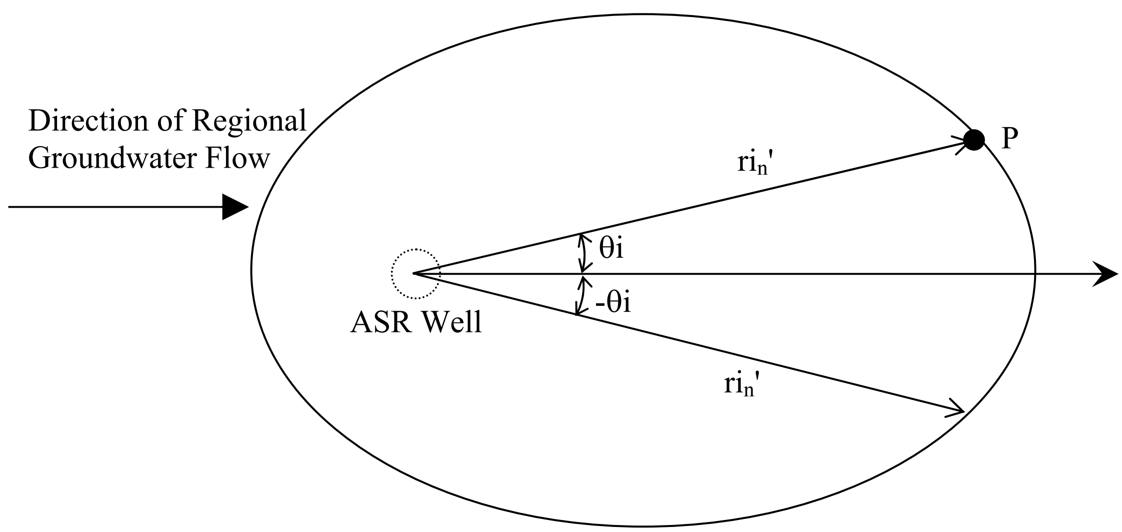

Figure 3-5. Position and shape of the interface after injection period (t=Ti).

Figure 3-5 illustrates a typical position and shape of the interface after injection period ($t=T_i$), where:

P = Point on the front separating the injected water from the ambient water

(ri_n', θi) = Polar coordinate of point P at the end of injection phase

At the end of recharge period ($t=T_i$), comprised of **n** discrete time steps, the coordinate of point P will be (ri_n', θi). Often, following the injection phase, there is a storage period. After a known time of storage, $\mathbf{T_s}$, and under natural gradient condition, it is assumed that the volume of stored water is displaced down gradient a distance $\mathbf{B_s}$ from the center of the ASR well.

$$B_s = \frac{qT_s}{\eta} \qquad (3\text{-}15)$$

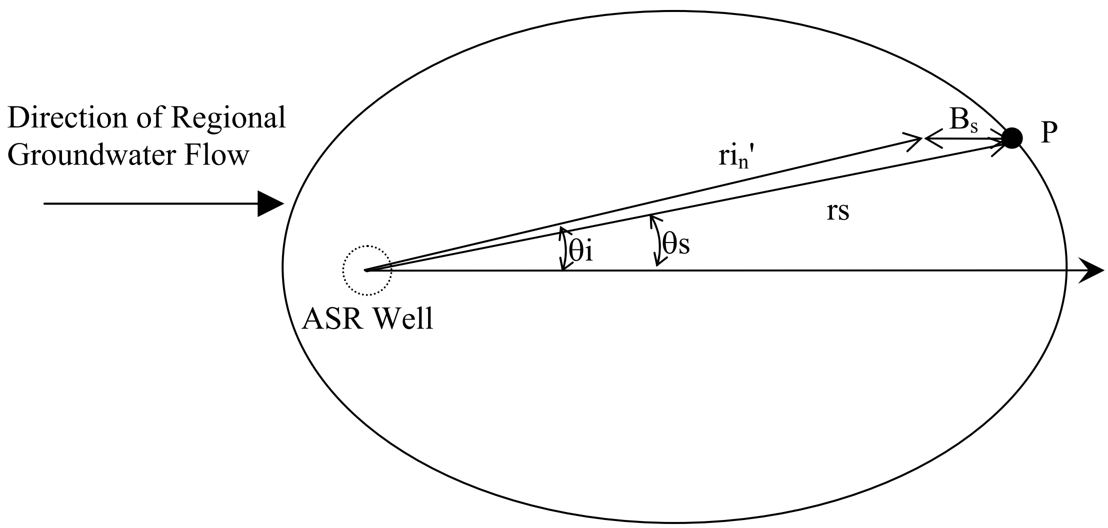

Figure 3-6. Position and shape of the interface after storage period (t=Ti+Ts).

At the end of the storage period, extraction takes place in the same ASR well. Figure 3-6 shows the starting of extraction phase (end of storage). In Figure 3-6, **rs** is the distance of point **P** from the well at the end of storage. The concentrations of water quality parameters such as chloride in the recovered water vary between that of ambient water of the aquifer and the recharge water. Similar to the injection period, the movement of fresh water is analyzed in small time increments of **Δt**.

Assuming that $\mathbf{Q_r}$ is the extraction flow rate of the ASR well, the radial extent of the water recovered is given by equation (3-16):

$$A = \left(\frac{Q_r \Delta t}{L \eta \pi} \right)^{\frac{1}{2}} \tag{3-16}$$

Where **A** is the radial extent of the cylinder of water recovered from the ASR well, [L]; **Δt** is the duration of the time interval, [T]; and $\mathbf{Q_r}$ is the extraction flow rate during the recovery phase [L^3/T].

After pumping this volume, the plan view of freshwater may be depicted as in Figure 3-7, where the shaded area in this figure represents the area of recovered water, $\pi \mathbf{A^2}$.

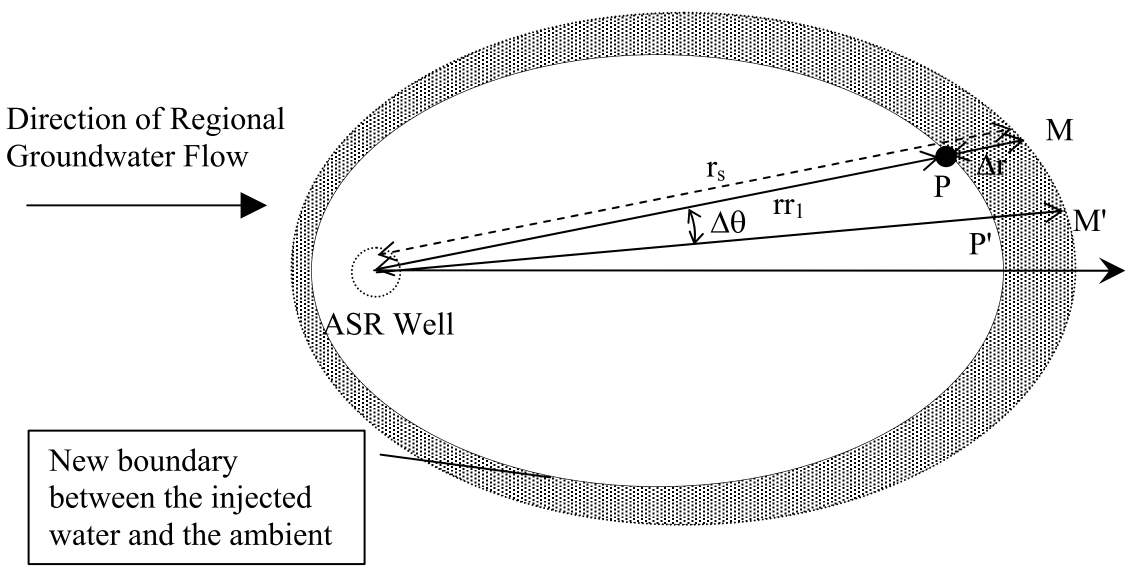

Figure 3-7. Position and shape of the interface at the beginning of the recovery phase.

In Figure 3-7, $\mathbf{rr_1}$ equals to the new distance of point **P** from the center of injection well:

$$rr_1 = rs - \Delta r$$

For a small value of Δθ it can be assumed that arcs **PP'** and **MM'** define circles. Thus:

$$\pi(rs^2 - rr_1^{\ 2})\frac{\Delta\theta}{360} = \pi A^2 \frac{\Delta\theta}{360} \tag{3-17}$$

$$\therefore \qquad rr_1 = \sqrt{rs^2 - A^2} \tag{3-18}$$

During the recovery time, **Δt**, the volume of stored water is displaced down gradient a distance $\mathbf{B_r}$ from the center of the ASR well.

$$B_r = \frac{q\Delta t}{\eta} \tag{3-19}$$

Similar to equations (3-6) and (3-10), the distance of point **P** from the injection well is equal to $\mathbf{rr_1'}$ where:

$$rr_1' = \sqrt{rr_1^2 + B_r^2 + 2rr_1 B_r \cos\theta s} \tag{3-20}$$

$$\theta_{new} = \theta s - Arc\sin(\frac{B_r}{rr_1'}\sin\theta s) \tag{3-21}$$

According to Figure 3-7, all the recovered water is injected freshwater; hence the concentration is the same as the concentration of injected water. But if recovery continues, some particles on the circumference of the freshwater body will reach the extraction well. From this moment, the concentration of dissolved solutes (i.e. chloride) in the recovered water is no longer at concentrations of the injected water.

The first particle on the injected/ambient water interface that reaches the well is always located at θ=π. After that, the target solute concentrations in the recovered water depend on the relative fractions of injected water and ambient water surrounding the well.

Figure 3-8 shows the front positions at two different times during recovery. At every time increment an angle θ can be determined where the value of $\mathbf{rr_n=0}$. The fraction of ambient groundwater in the water recovered from ASR well is then calculated as:

$$F = \frac{\psi}{360} \tag{3-22}$$

where:

$$\psi = 2(\pi - \theta) \tag{3-23}$$

The concentration of recovered water is then calculated from equation (3-24):

$$C_R = FC_A + (1-F)C_I \tag{3-24}$$

In equation (3-24), $\mathbf{C_A}$ is concentration of ambient water [M/L^3] and $\mathbf{C_I}$ is concentration of injected water [M/L^3].

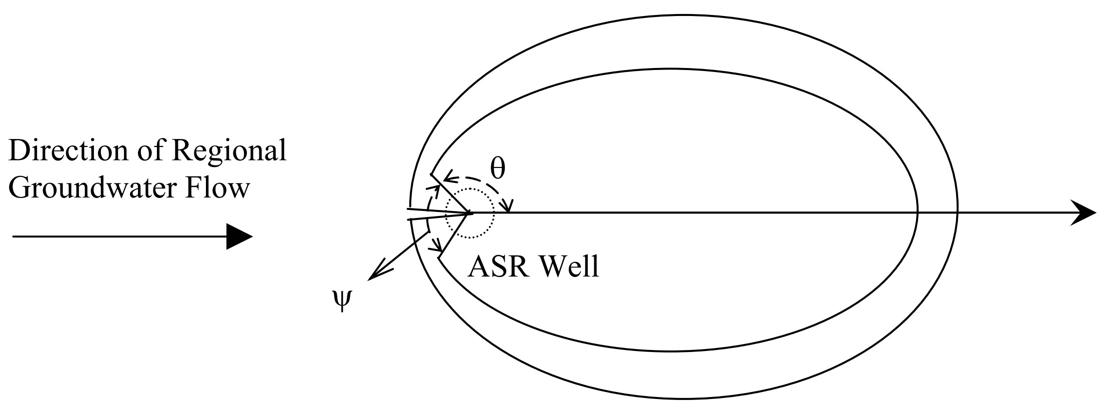

Figure 3-8. Position of the interface at two different times during recovery.

Usually there is a storage time at the end of each cycle and then a new cycle of injection, storage, and recovery begins. The coordinate system of each point at the end of first cycle will be the initial coordinate for the second cycle. This process continues for the other cycles during operation of the ASR system.

Based on the equations (3-1) to (3-24), a FORTRAN program was developed to simulate the concentration of recovered water during the recovery phase of an ASR system. The program requires one input file containing data on the number of cycles, the target solute concentration of injected water (C_I), the target solute concentration of ambient water (C_A), the aquifer hydraulic conductivity (K), the thickness of the aquifer (L), the effective porosity of the aquifer (η), and the hydraulic gradient in the aquifer ($\frac{d\varphi}{ds}$). In addition, for each individual cycle, the model input file requires: the injection time (T_i), the storage time (T_s), the total recovery time (T_r), the storage time at the end of each cycle (T_d), the number of time subintervals for each phase (n), the injection flow rate (Q_i), and the recovery flow rate (Q_r).

Validation of the Quasi-analytical Model using Numerical Model

A one-layer groundwater flow model was constructed using MODFLOW-96 (Harbaugh and McDonald, 1996) and MT3DMS (Zheng and Wang, 1998) to simulate the movement of the injected bubble in the aquifer and to compare the concentration of recovered water from this model with the values obtained from the quasi-analytical model. The input data for both models are from the engineering report for the Boynton Beach monitoring ASR site in Florida, prepared by CH2M HILL Southeast, Inc. in 1993. Aquifer properties are taken from USGS Water-Resources Investigations Report No. 02-4036 (Reese, 2002).

Table 3-1 shows the duration and flow rates for different phases of operation at this site. Data are available for three cycles of injection, storage, and recovery.

Transmissivity was estimated from the analysis of the recovery of water level after a period of constant rate pumping during a packer test, and it was reported to be 9400

ft^2/day. The thickness of the aquifer in the storage zone is 105 ft. Thus, the average horizontal hydraulic conductivity is equal to 89.52 ft/day. Ambient water quality data were collected from storage and monitoring wells. The chloride concentration of ambient water at this site was about 1950 mg/L and for the injected water it was reported to be 50 mg/L. Aquifer porosity is reported to be 0.3 for this site.

Table 3-1. Duration and flow rates for three cycles of ASR operation in Boynton Beach, Florida.

	Cycle 1	Cycle 2	Cycle 3
Injection Time (day)	12.690	41.376	41.547
Storage Time (day)	0.130	0.010	8.768
Recovery Time (day)	6.981	15.979	21.750
Delay Time (day)	1.000	18.543	---------
Injection Flow Rate (ft^3/day)	131140.6	181875.7	179629.6
Injection Flow Rate (ft^3/day)	183408.6	144955.7	195192.3

The numerical model consists of 101 columns and 101 rows and one confined layer with the thickness of 105 ft. A regular grid spacing of 10 ft is used for each row and column. The horizontal hydraulic conductivity of this layer is 89.52 ft/day and storativity is set to 0.0005. The effective porosity is 0.3. The flow field was first calculated with MODFLOW. The 3rd-order TVD scheme (Ultimate) with Courant number 0.75 was used in the simulation for the advection term and the GCG solver is used to solve the system equations. No dispersion is considered in the model. To obtain the desired hydraulic gradient, the cells in the first and last columns of the model are specified as fixed-head boundaries. Water of a constant concentration, C_I, is injected into the well at the cell [51, 51, 1]. The initial concentration, C_B, is set to 1950 mg/L. Eleven stress periods are simulated for three cycles of ASR operation and a transient flow is performed for the length of 168.774 days (Total operation time). The total simulation time for the numerical model was about ten minutes while it takes less than one minute to run the FORTRAN code for a one-layer model.

Figure 3-9 shows the position of the front and contour map of the concentration field with the natural gradient of 0.01 at time=18.55 days, which is close to the end of recovery phase in the first cycle. This figure may be compared to Figure 3-8 of the analytical model.

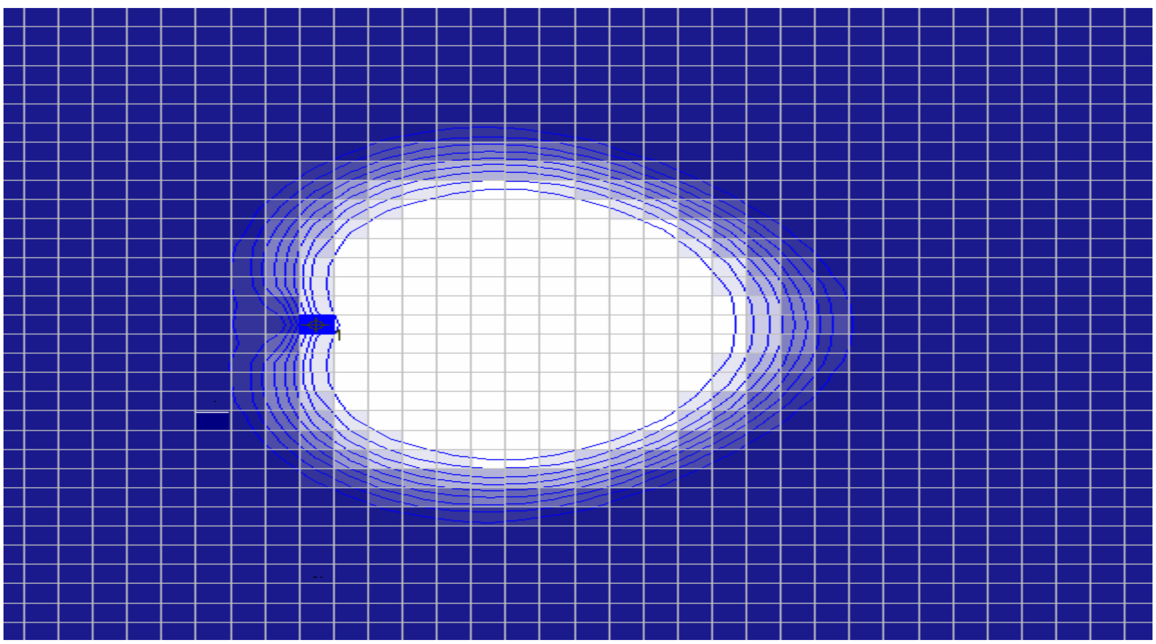

Figure 3-9. The front position at time=18.55 days.

Figure 3-10 shows the concentration breakthrough curves at the injection/extraction well for three different background gradients of 0.1, 0.2, and 0.3 from numerical and quasi-analytical simulations. The results match showing that quasi-analytical model performed well. Considering the relatively short execution times required by the quasi-analytical model, one may be surmised it could serve as a good alternative model to MODFLOW/MT3DMS for simulating the performance of ASR systems.

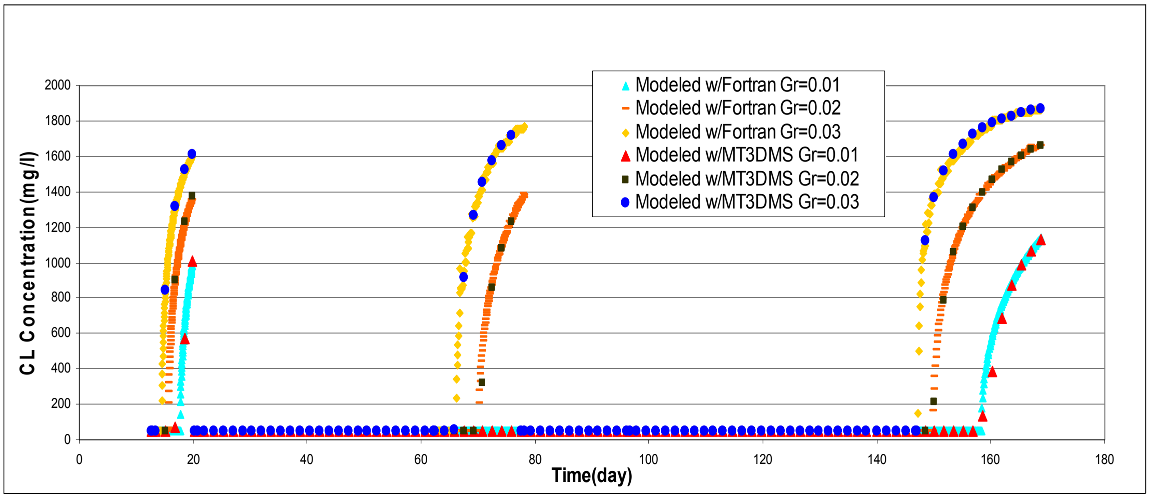

Figure 3-10. Concentration of recovered water obtained from numerical and analytical models.

Developing the Model for Multiple Layers

Several assumptions were made to expand the utility of the one layer model such that applications of ASR systems installed in stratified aquifers could be examined. These assumptions included:

- the absence of water movement between layers;
- a constant horizontal head gradient($\frac{d\varphi}{ds}$) in all layers; and,
- layer specific injection and extraction flow rates which are proportional to transmissivity of each layer.

Given unit thickness for each layer, the average of hydraulic conductivity of the aquifer is:

$$K_{ave} = \frac{\sum_{1}^{NL} K_i}{NL} \qquad (3\text{-}25)$$

K_i= Hydraulic conductivity of the **i**th layer in the aquifer [L/T]; and

NL= Number of layers in the aquifer

The transmissivity of **i^th^** layer is defined product the **i^th^** layer hydraulic conductivity [L/T] and layer thickness. Therefore, the transmissivity of the **i^th^** layer is equal to

$$T_i = K_i \cdot L_i \tag{3-26}$$

where L_i is layer thickness, [L]. The total transmissivity of the aquifer, T_{total}, then equals:

$$T_{total} = K_{ave} \cdot L \tag{3-27}$$

in which **L** is the thickness of the aquifer [L]; hence,

$$T_{total} = \sum_{1}^{n} T_i \tag{3-28}$$

The injection and recovery rates for the **i^th^** layer are calculated from equations (3-29) and (3-30):

$$Q_{Ii} = \frac{T_i}{T_{total}} Q_I \tag{3-29}$$

$$Q_{Ri} = \frac{T_i}{T_{total}} Q_R \tag{3-30}$$

By defining

$$\lambda_i = \frac{T_i}{T_{total}} \tag{3-31}$$

and

$$\gamma_i = \frac{L_i}{L} \tag{3-32}$$

then equations (3-29) and (3-30) reduce to:

$$Q_{Ii} = \lambda_i Q_I \tag{3-33}$$

$$Q_{Ri} = \lambda_i Q_R \tag{3-34}$$

From equations (3-3) and (3-16), it was seen in a single layer that the two-dimensional horizontal geometry of injected water varied as a function of natural gradient and the injection/recovery flow rates. Therefore, the radial extent of the cylindrical volume of injected water for the **ith** layer is $\mathbf{C_i}$ and is equal to:

$$C_i = \left(\frac{Q_{Ii}\Delta t}{L_i \eta \pi}\right)^{\frac{1}{2}} = \left(\frac{\lambda_i Q_I \Delta t}{L_i \eta \pi}\right)^{\frac{1}{2}} \qquad (3\text{-}35)$$

And in using the definition of $\boldsymbol{\gamma_i}$, will have:

$$C_i = \left(\frac{\lambda_i Q_I \Delta t}{\gamma_i L \eta \pi}\right)^{\frac{1}{2}} \qquad (3\text{-}36)$$

Similarly, equation (3-16) converts to:

$$A_i = \left(\frac{\lambda_i Q_R \Delta t}{\gamma_i L \eta \pi}\right)^{\frac{1}{2}} \qquad (3\text{-}37)$$

The horizontal displacement B during time $\mathbf{\Delta t}$ for each layer is a function of constant hydraulic gradient and layer specific hydraulic conductivity; thus,

$$B_i = \frac{-K_i \frac{d\varphi}{ds}\Delta t}{\eta} \qquad (3\text{-}38)$$

Therefore, $\mathbf{C_{Ri}}$, the concentration of the target solute in water recovered from each layer can be estimated. The total concentration of target solute is the summation of flow-weighted concentrations from all layers:

$$C_{Rtotal} Q_R = \sum_{1}^{NL} C_{Ri} Q_{Ri} \qquad (3\text{-}39)$$

From equation (3-29) and (3-30) and (3-39) the following is obtained:

$$C_{Rtotal} = \sum_{1}^{NL} \lambda_i C_{Ri} \quad (3\text{-}40)$$

Modeling the Distribution of Hydraulic Conductivity in the Aquifer

The geometry of the subsurface plume of injected freshwater is influenced by the aquifer properties and variation in hydraulic conductivity within the aquifer. In addition, dispersion and mixing between the injected water and native water are also related to the distribution of permeability within the storage zone

The dispersivity in a stratified aquifer was discussed by Gelhar (1993) and Dagan (1994). A very simple description of mixing process in a heterogeneous aquifer can be developed if we assume that the aquifer exhibits perfect stratification, in the sense that horizontal hydraulic conductivity varies vertically through the depth of the aquifer (Gelhar, 1993). The values of hydraulic conductivity can be modeled as a random space function to account for their spatial variability and usually their logarithm tends to be normally distributed (Dagan, 1994).

Theory

A lognormal variant such as hydraulic conductivity will have a mean value of ***m*** and standard deviation ***σ*** and is expressed in brief form as ***L: (m, σ)***. Similarly a normal variant (such as log transformed conductivities) will have a mean ***m'*** and standard deviation ***σ'*** which is expressed by ***N: (m', σ')***. The lognormal variant is related to the normal variant by the following equation:

$$L:(m,\sigma) = \exp(N:(m',\sigma')) \quad (3\text{-}41)$$

The relationship between means and standard deviations of normal and lognormal distributions is as follow (David, 1977):

$$\sigma^2 = m^2(\exp(\sigma'^2) - 1) \quad (3\text{-}42)$$

and

$$m = \exp(m' + \frac{\sigma'^2}{2}) \tag{3-43}$$

In these equations, both ***m*** and ***σ*** are known (***m*** is the average hydraulic conductivity and ***σ*** is manifestation of the apparent aquifer dispersivity).

Previously it was stated that the total transmissivity of the aquifer was defined as the average hydraulic conductivity [L/T] times the thickness of the aquifer [L]:

$$T_{total} = K_{ave} \cdot L \tag{3-44}$$

From equation (3-44) an appropriate mean value for the average hydraulic conductivity may be determined assuming the thickness of the aquifer and total transmissivity are known. If in addition a suitable value for variance of lognormal distribution can be estimated from the apparent aquifer dispersivity, then, equations (3-42) and (3-43) may be used to derive values of the mean (**m'**) and the standard deviation (**σ'**) for normal deviate of log transform hydraulic conductivity.

The probability density function (PDF) curve representing this normal distribution is a function of ***m'*** and ***σ'***.

$$f(x) = \frac{1}{\sigma'\sqrt{2\pi}} \exp\left[-\frac{1}{2}\left(\frac{x - m'}{\sigma'}\right)^2\right] \tag{3-45}$$

This curve is symmetrical about the mean value (**m'**). Figure 3-11 shows a sample curve of normal distribution with mean and standard deviation values of 2.

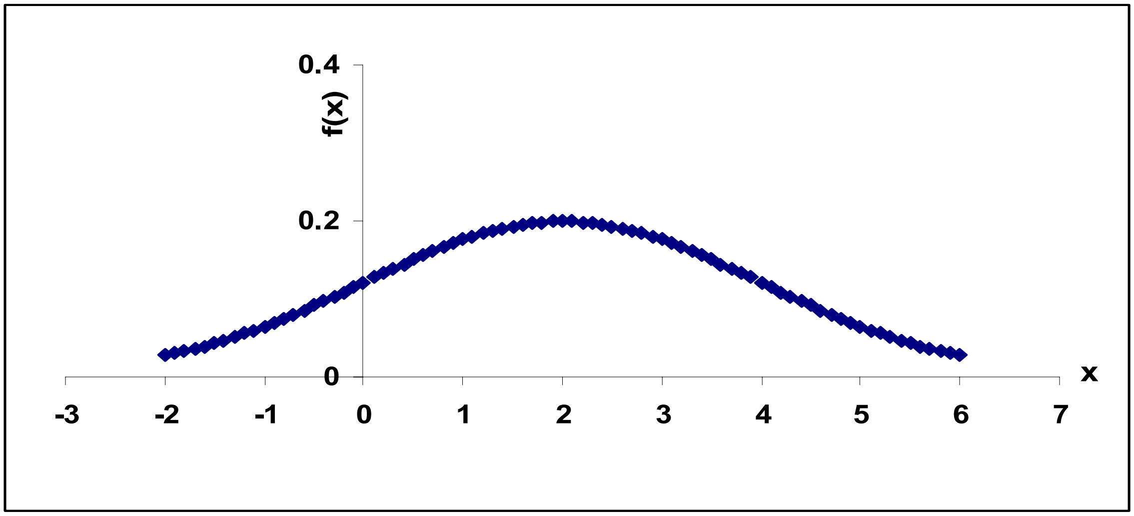

Figure 3-11. Probability Density Function for the Normal Distribution, N: (2, 2)

For each value of the normal deviate ***x***, there is an associated density of probability ***f(x)*** and the probability of one value lying between ***x*** and ***x+dx*** will be ***f(x) dx***. Consequently, the probability of ***x*** lying between ***a*** and ***b*** will be equal to:

$$prob\{a \leq x \leq b\} = \int_a^b f(x)dx \qquad (3\text{-}46)$$

And this integral, if extended from **-**∞ to +∞ is also equal to:

$$prob\{-\infty \leq x \leq +\infty\} = \int_{-\infty}^{+\infty} f(x)dx = 1 \qquad (3\text{-}47)$$

The probability of x being smaller than or equal to a given value of $\boldsymbol{x_0}$ is called the cumulative probability, $\boldsymbol{F(x_0)}$, and is equal to:

$$F(x_0) = prob\{x \leq x_0\} = \int_{-\infty}^{x_0} f(x)dx \qquad (3\text{-}48)$$

By the definition, cumulative probability can be written as:

$F(-\infty) = 0$ and $F(+\infty) = 1$ (3-49)

The integral $\int_{-\infty}^{x_0} f(x)dx$ for a normally distributed deviate is not easily solved.

Below is an approximation and was used herein to generate a normal distribution of log-transformed hydraulic conductivities that were then used to simulate water quality changes in recovered water from an ASR well located in stratified aquifer:

$$F(x_0) = 0.5\left[1 + \left\{1 - \exp\left(-2\left(\frac{x_0 - m'}{\sigma'}\right)^2 \Big/ \pi\right)\right\}^{\frac{1}{2}}\right] \qquad (3\text{-}50)$$

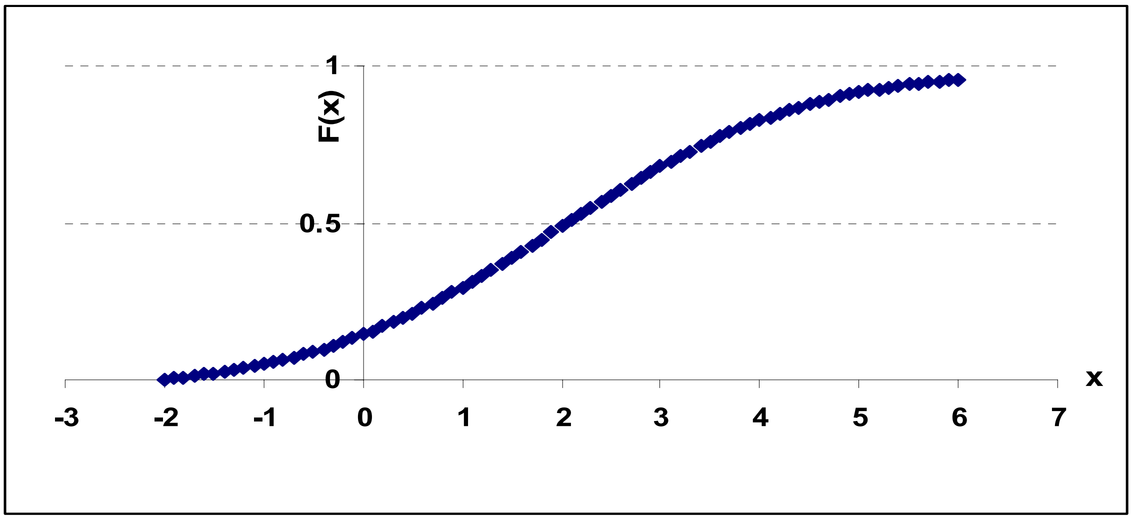

Figure 3-12. Cumulative probability function, $F(x_0)$, for N: (2, 2).

Figure 3-12 shows the cumulative probability function, $\boldsymbol{F(x_0)}$, for **N: (2, 2)**. To generate a suite of hydraulic conductivities that are then used to characterize a uniformly layered aquifer, it is necessary that the conductivity assigned to each layer reflect a fraction of aquifer thickness that honors the assumed underlying log-normal conductivity distribution; hence, equation (3-50) is first rearranged to give $\boldsymbol{x_0}$:

$$x_0 = m' + \sigma'\sqrt{-0.5\pi Ln\left(1 - \left(2F(x_0) - 1\right)^2\right)} \qquad (3\text{-}51)$$

Next, $\boldsymbol{F(x_0)}$ is incrementally increased by $\boldsymbol{\Delta F(x_0)}$ from 0 and 1, where the value of $\boldsymbol{\Delta F(x_0)}$ is equal to fraction of total aquifer thickness represented by a single layer. From each value $\boldsymbol{F(x_0)}$ a unique conductivity value of $\boldsymbol{x_o}$ is estimated from equation (3-51). The resultant hypothetical aquifer will then have a lognormal distribution of conductivities with the mean conductivity of $\boldsymbol{m}$ and standard deviation of $\boldsymbol{\sigma}$.

Sensitivity Analysis and Comparison of the Results from Analytical Model with the Real ASR Performance Data

Figure 3-13 shows the results from the FORTRAN code based on the ASR data from a site in Boynton Beach, Florida. It is assumed that aquifer is made of 100 layers, with different hydraulic conductivities which are lognormally distributed through the depth of the aquifer. Mean value of hydraulic conductivity (***m***) is equal to transmissivity of the aquifer divided by thickness. The value of the standard deviation (σ) is adjusted to simulate the apparent dispersion in the aquifer, based on ASR results. Higher values of the standard deviation will result in greater apparent dispersion at the ASR well during the recovery phase. As a result, target solutes concentrations will appear to increase sooner during the recovery phase than with a smaller value of (σ).

Altering the value of natural gradient can also bring about a change in the solute breakthrough that is similar to changes effected by adjusting (σ). In general, an increase in the hydraulic gradient produces premature solute breakthrough.

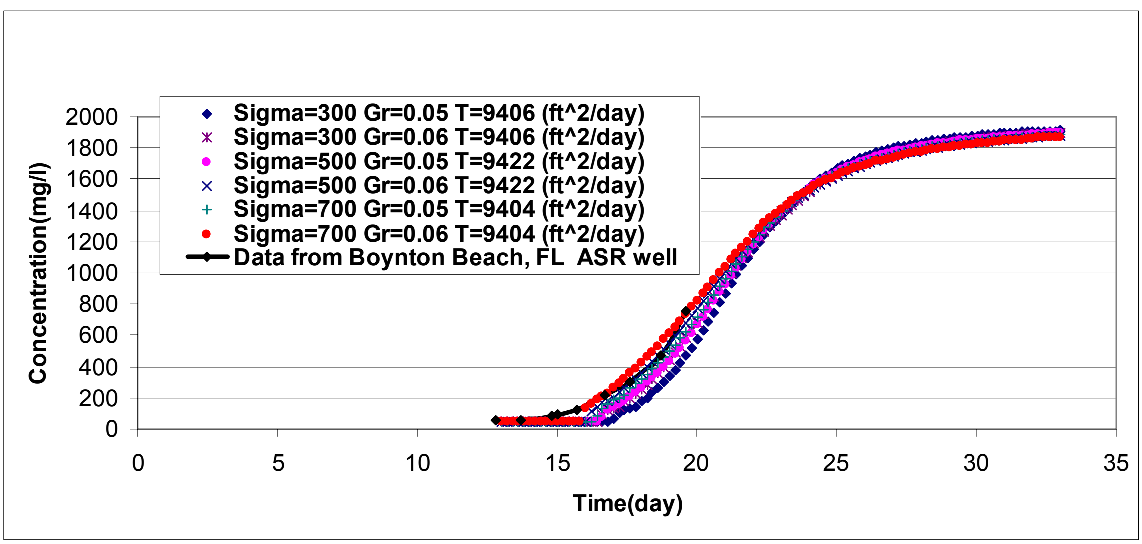

Figure 3-13. Sensitivity analysis for the analytical results from the FORTRAN code

Figure 3-14 shows the results from the model with the real ASR performance data during two cycles of ASR operation. By calibrating the model to the first cycle data we can get an estimation of our variable parameters in the aquifer and then use them for other cycles. The best fitting line takes place when natural gradient is 0.06 and standard deviation is equal to 500. Figure 3-14 indicates that analytical model performs well in predicting extracted water quality during subsequent extraction cycles.

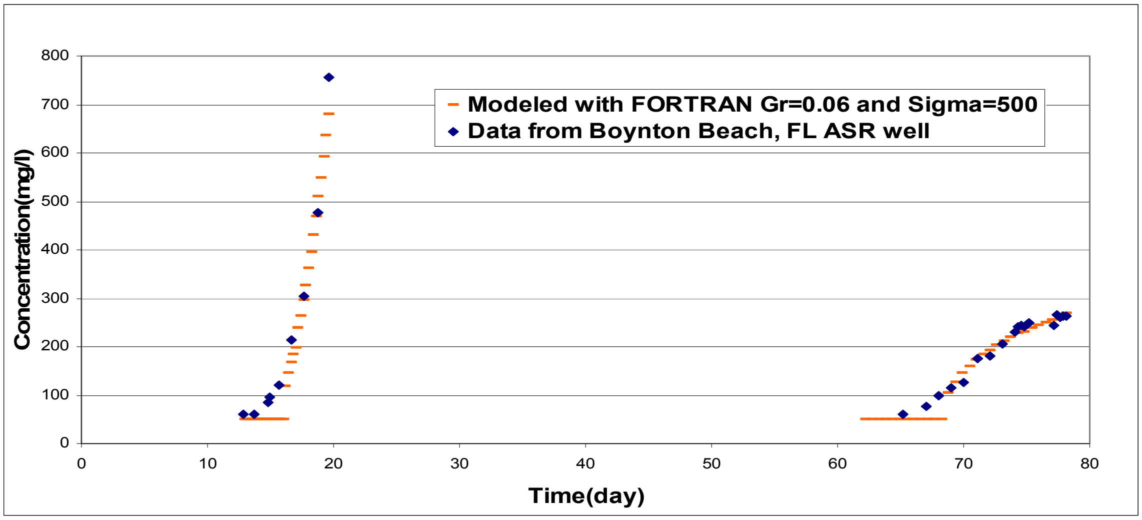

Figure 3-14. Comparison of the analytical model results with the real ASR performance data.

CHAPTER 4
CONCLUSIONS AND RECOMMENDATIONS

Simulation results from the quasi-analytical model reproduced water quality simulations obtained using well known numerical models. Considering the relatively short execution times required by the quasi-analytical model and the quality of model validation results, it is concluded that the model developed herein is a good alternative to MODFLOW/MT3DMS for simulating the performance of ASR systems. In addition, given the minimal input data required, the quasi-analytical model is easier to apply than many existing numerical models.

The groundwater flow modeling showed that the natural hydraulic gradient in the aquifer is of great importance in the operation of an ASR system and must be considered to achieve the desired extraction water quality. Maximum100% recovery efficiency is not viable unless the hydraulic gradient does not exist or is close to zero.

To emulate the effects of hydrodynamic dispersion, simulations were performed as if the aquifer were stratified and the horizontal hydraulic conductivity varied vertically in a statistically defined manner. By calibrating the model to the water quality data from pilot tests performed at Boynton Beach, Florida, estimations of model parameters were obtained. The model parameters calibrated included the natural hydraulic gradient and the variance of hydraulic conductivity. Following calibration, the quasi-analytical model performed well in predicting the extracted water quality during subsequent extraction cycles of the pilot ASR system.

This model could be used to optimize the operation of ASR systems. For instance, increasing recovery flow rate could increase recovery efficiency.

Anisotropy within an aquifer will cause the geometry of freshwater stored in the subsurface to be irregular. This can greatly affect the extracted water quality. The current model does not address this anisotropy. Thus, it has a limitation in predicting water quality and cannot be applied in the presence of this irregularity.

Future research could include developing the quasi-analytical model for a system of multiple ASR wells. Design of ASR systems, like other engineering design processes, is a sequence of decisions between alternatives under conditions of uncertainty. Short-term injection tests in pilot projects, coupled with regional studies and modeling tools, are crucial to assess the feasibility of using ASR in a much larger scale as proposed in CERP.

LIST OF REFERENCES

Ahlfeld D. P., 1999, Advective Control of Groundwater Contaminant Plumes: Model Development and Comparison to Hydraulic Control. Water Resources Research 35, no. 8, pp 2285-2293.

American Society of Civil Engineers, 2001. Standard Guidelines for Artificial Recharge, EWRI/ASCE 34-01.

Arthur J. D., Cowart J. B., Dabous A., 2001, Florida Aquifer Storage and Recovery Geochemical Study: Year Three Progress Report. Florida Geological Survey, Open File Report No. 83, p. 46.

Bear J, 1979, Hydraulics of Groundwater. McGraw-Hill, New York, pp 276-299.

Bouwer H., 1996, Issues in Artificial Recharge. Water Science and Technology 33, no. 10-11.

Bouwer H., 2002, Artificial Recharge of Groundwater: Hydrology and Engineering. Journal of Hydrology 10, pp 121-142.

CH2M Hill Southeast, Inc, June 1993, Engineering Report for the Boynton Beach Aquifer Storage and Recovery System. Report SEF26410.Q1.

Dagan, G., 1994, An Exact Nonlinear Correction to Transverse Macrodispersivity for Transport in Heterogeneous Formations. Water Resources Research 30, no. 10, pp 2699-2705.

David M, 1977, Geostatistical Ore Reserve Estimation. Elsevier Scientific Publishing Company, Amsterdam, pp 7-18.

Evans M, Hastings N, Peacock B, 2000, Statistical Distributions. John Wiley and Sons, Inc, New York, pp 129-133, 145-150.

Gelhar, L. W., 1993, Stochastic Subsurface Hydrology. Prentice-Hall, Englewood Cliffs, N.J, pp 204-207.

Guo W., Langevin C. D., 2002, User's Guide to SEAWAT: A Computer Program for Simulation of Three-Dimensional Variable-Density Ground-Water Flow. USGS, Techniques of Water-Resources Investigations 6-A7, Tallahassee, Florida, pp 75.

Harbaugh A. W., McDonald M. G., 1996a, User's Documentation for MODFLOW-96, an Update to the U.S. Geological Survey Modular Finite-Difference Ground-Water Flow Model. USGS Open-File Report 96-485.

Harbaugh A. W., McDonald M. G., 1996b, Programmer's Documentation for MODFLOW-96, an Update to the U.S. Geological Survey Modular Finite-Difference Ground-Water Flow Model. USGS Open-File Report 96-486.

Javandel, I., Doughty, C., and Tsang, C., 1984, Groundwater Transport: Handbook of Mathematical Models. American Geophysical Union, Washington, D.C., pp 35-67.

Javandel, I., Tsang, C., 1986, Capture-Zone Type Curves: A Tool for Aquifer Cleanup. Ground Water 24, no. 5, pp 616-625.

Lloyd J. W., June 2001, Groundwater Vulnerability and the Reuse of Water, With Reference to Saudi Arabia. International Journal of Water Resources Development 17 (2), pp 179-184.

Martin J. B., Dean R. W. September 2001. Exchange of Water between Conduits and Matrix in the Floridian Aquifer. Chemical Geology 179, pp 145-165.

McDonald M. G., Harbaugh A. W., 1988, MODFLOW, a Modular Three-Dimensional Finite Difference Ground-Water Flow Model. USGS Open-File Report 83-875, Chapter A1.

Merritt M. L., 1985, Subsurface Storage of Freshwater in South Florida: A Digital Model Analysis of Recoverability. U. S. Geological Survey Water-Supply Paper 2261, p 44.

Missimer T. M., Walker CW, Bloetscher F, September 1992, Use of Aquifer Storage and Recovery Technology to Improve Membrane Water-Treatment Plant-Efficiency, Collier County, Florida. Desalination. Elsevier Science BV, Amsterdam, pp 269-280.

Missimer T. M., Guo W, Walker CW, Maliva RG, February 2002, Hydraulic and Density Considerations in the Design of Aquifer Storage and Recovery Systems. Florida Water Resources Journal, pp 30-35.

Muniz A. and Ziegler W. B., July 1994, Aquifer Storage and Recovery in Southeast Florida. Artificial Recharge of Groundwater, II: Proceeding of the Second International Symposium on Artificial Recharge of Groundwater, Published by the ASCE, New York 10017-2398, pp 311-323.

Muskat M, 1937, The Flow of Homogeneous Fluids Through Porous Media. McGraw-Hill, New York, 763 pp.

Nelson, R. W., 1978, Evaluating the Environmental Consequences of Groundwater contamination. 2, Obtaining Location/Arrival Time and Location/Outflow Quality Distribution for Steady Flow Systems. Water Resources Research 14, no. 3, pp 416-428.

Nguyen P. D. and Mueller T. K., December 1996, A Cautious Look at Aquifer Storage Recovery in South Florida from a Public Health Viewpoint. Florida Water Resources Journal, pp 24-27. Available: www.fwrj.com/articles/9612.pdf.

Pyne D. G., July 1994, Seasonal Storage of Reclaimed Water and Surface Water in Brackish Aquifers Using Aquifer Storage Recovery (ASR) Wells. Artificial Recharge of Groundwater, II: Proceedings of the Second International Symposium on Artificial Recharge of Ground Water, Published by the ASCE, New York 10017-2398, pp 282-298.

Pyne, D. G., February 2002, Aquifer Storage Recovery Wells: The Path Ahead. Florida Water Resources Journal, pp 19-22, 27.

Pyne, D. G., ASR Systems, 2003, http://www.asrforum.com, July 26, 2003.

Reese R, 2002, Inventory and Review of Aquifer Storage and Recovery in Southern Florida. U.S. Geological Survey, Water-Resources Investigations Report 02-4036, 55 pp.

Zheng C, Wang P. P., 1999, MT3DMS: A Modular Three-Dimensional Multispecies Model for Simulation of Advection, Dispersion and Chemical Reactions of Contaminants In Groundwater Systems; Documentation and User’s Guide, Contract Report SERDP-99-1, U.S. Army Engineer Research and Development Center, Vicksburg, MS, University of Alabama, 168 pp.

BIOGRAPHICAL SKETCH

Ali Sedighi was born in 1975 in Tehran, Iran. He received a mathematics and physics diploma from Sadegh High School in 1993. In February, 1998, Ali graduated from Sharif University of Technology with a Bachelor of Science in civil engineering. He enrolled in the graduate school at the University of Florida in fall of 2001. He joined the Master of Engineering program in the Department of Civil and Coastal Engineering under the guidance of his major professor, Dr. Kirk Hatfield.